



Process optimisation and structural insights on single-atom tungsten catalyst production under varied annealing with tungsten precursor

Hanna Ilyani Zulhaimi ^a, Subash C.B. Gopinath ^{b,c *}, and Farizul Hafiz Kasim ^a

^aFaculty of Chemical Engineering & Technology, Universiti Malaysia Perlis (UniMAP), 02600 Arau, Perlis, Malaysia

^bDepartment of Neonatology, Saveetha Medical College & Hospital, Saveetha Institute of Medical and Technical Sciences (SIMATS), Thandalam, Chennai 602 105, Tamil Nadu, India

^cInstitute of Nano Electronic Engineering, Universiti Malaysia Perlis (UniMAP), 01000 Kangar, Perlis, Malaysia

*Corresponding author. Tel.: +601110472006; e-mail: subash@unimap.edu.my

Received 03 September 2025, Revised 17 September 2025, Accepted 24 September 2025

ABSTRACT

The precise control of a single atomic site has been a significant concern in the field of single-atom catalysts. However, research on the effect parameters or factors that influence the matrix material is limited, yet it plays a crucial role in understanding how single-atom catalysts behave. In this study, one of the key parameters for synthesising a single-atom tungsten catalyst is discussed to optimise the yield of an active site. Variations in the involved parameters, such as the stoichiometry ratio, annealing temperature, annealing duration, tungsten complex ion formation, and rapid mixing of tungsten to produce the precursor, were examined. The stoichiometric ratio was set at Pt: W with a 17:1 ratio. Alkali treatment was applied after annealing to remove oxide by-products and to promote electronic delocalisation for single-atom formation. X-Ray diffraction (XRD) spectra showed that the structure of Pt displayed peaks at 39.7°, 67.5°, and 46.1°, while peaks for W₂C were observed at 40° and 46°, and WC spectra showed a peak at 84°. Variations in reaction time during tungsten complex ion formation led to changes in crystal phases caused by the formation of tungsten alkoxide, which affects the growth of crystallinity and the altered aggregation pattern. XRD results indicated that annealing at 650°C and 700°C for 2 hours likely facilitated the formation of a single-atom tungsten catalyst. The volume of methanol used during the reaction on tungsten complex ions showed that 10 mL provided better formation of tungsten alkoxide, especially with sonication mixing for 30 seconds. The durations of tungsten alkoxide formation revealed that 10 and 15 minutes yielded the best reaction times, characterised by low intensity and broader peaks. A template synthesis for the single-atom catalyst is reported to aid understanding.

Keywords: Single-atom catalyst, Bottom-up approach, Micromixing, Metal ion complexes, Annealing process, XRD analysis

1. INTRODUCTION

Catalysts are essential in chemical processing, promoting a sustainable manufacturing pathway [1, 2]. The development of advanced materials, especially for electrochemical reactions, relies heavily on materials vital to industry. Most chemical processes critically depend on a catalyst's activity, selectivity, and stability, which affect its overall performance, efficiency, and system effectiveness. Currently, the use of advanced materials depends on expensive and limited resources, such as platinum group metals (PGMs), including platinum (Pt), palladium (Pd), rhodium (Rh), iridium (Ir), ruthenium (Ru), and gold (Au) [3]. This not only raises the overall cost but also contributes to a complex carbon footprint, which is challenging to reduce and requires specialised equipment for refining.

At the molecular level, the catalytic reaction takes place on the surface or interface of a solid catalyst [3]. In this region, a minimum of reactants adsorbs onto the catalyst surface, which has coordination-unsaturated atoms, and is then converted into products that are eventually desorbed from the catalyst surface [4]. The surface atoms of solids are more coordination-unsaturated compared to their neighbouring or bulk atoms, granting them a unique selectivity capable of

turning over the catalytic cycle. Moreover, a unit associated with the surface of the solid catalyst is defined as an active site [5]. The structure and density of the active site influence the catalytic properties. Additionally, the pathway to catalytic activity depends on the geometric configuration and chemical bonding of the substrate on the surface [6]. The atomic and electronic structure of the interface determines this catalytic activity. The change in surface area for catalytic reactions enabled single-atom catalysts to demonstrate their capacity for interface manipulation.

According to Zhang and coworkers, who introduced the concept of single-atom catalysts (SACs), these catalysts are defined as those dispersed on support material, with isolated active sites that atomically activate the support [7]. This advances scientific research in multiphase catalysis down to the monatomic level [8]. The distinctive feature of SACs, which are uniformly distributed on the support material and have uncoordinated active site bridges, underpins the idea of a model system capable of functioning as both a heterogeneous and a homogeneous catalyst [9]. Therefore, SACs operate by maximising chemical reaction efficiency through 100% atomic utilisation [10]. Since SACs are fully active, they promote higher turnover or selectivity in reactions, thereby improving the overall system.

However, the investigation of variables that contribute to SACs synthesis is limited due to the multiple fabrication strategies employed. Additionally, this can control the variables and identify the factors that contributed to SACs development. Consequently, research into single-atom catalysts continues to progress, seeking to overcome limitations in both heterogeneous and homogeneous catalysis and to harness their potential in catalysis.

2. MATERIALS AND METHODS

2.1. Chemicals

Tungsten (IV) hexachloride (99.99% trace metal basis) and Vulcan carbon black XC72R were obtained from Fuel Cell Store. Methanol (99.8%) ACS reagent and potassium chloride (90%) flakes were sourced from a laboratory at the National Tsing Hua University, Taiwan. All chemical reagents used in this study were of analytical reagent grade.

2.2. Stoichiometric Ratio and Annealing Response to the Single-Atom Tungsten Growth

Vulcan black (Pt/C 20%) was used for this experiment and placed in an empty vial, while tungsten (IV) chloride was

prepared with a molar ratio of Pt:W = 1. The Vulcan black was sealed with parafilm to prevent spillage in a water bath. Sonication of Vulcan black lasted 1 hour. In a separate vial, tungsten (IV) chloride was mixed using a vortex mixer for 20 seconds, then dissolved in a methanol solution. After sonication, tungsten (IV) chloride was allowed to react for different periods (5, 10, 15, 20, and 60 minutes) before being combined with Vulcan black. After mixing, the mixture was dried on a hot plate at 60°C for one hour at ambient temperature. Prior to annealing, the RTA chamber was purged with argon and ammonia gases at a flow rate of 100 sccm, with a ramp rate of 10°C/min. After annealing, the sample underwent alkali treatment for 24 and 48 hours.

2.3. Stoichiometric Ratio and Annealing Response to the Single-Atom Tungsten Growth

The study investigated the reaction producing tungsten single-atom catalysts to observe the effect of tungsten metal complexes with methanol. The sample was then collected and subjected to an annealing process in a rapid thermal annealing (RTA) system at 650, 700, and 750°C, with annealing durations of 2 and 4 hours (Table 1). Reaction times were then tested at 5, 10, 15, 20, and 60 minutes. Additionally, the use of sonication was considered to aid

Table 1. Strategy for a single-atom tungsten catalyst for tungsten and annealing response

Precursor	Methanol (mL)	Reaction time (min)	Drying Condition	RTA						
				Ramp rate (°C/min)	Gas	Flow (sccm)	T (°C)	Time (hr)		
VB = 0.0504 g WCl ₆ = 0.0114 g	10	15	60°C, 1 hr	10	NH ₃	100	650	4		
							700			
	10	15		10		100	750			
							650	2		
							700			
							750			

Table 2. Strategy for a single-atom tungsten catalyst for tungsten and annealing response

Precursor	Methanol (mL)	Reaction time (min)	Drying Condition	RTA				
				Ramp rate (°C/min)	Gas	Flow (sccm)	T (°C)	Time (hr)
VB = 0.2000 g WCl ₆ = 0.0813 g	10	5	60°C, 1 hr	10	NH ₃	100	650	2
		10						
		15						
		20						

Table 3. Single-atom tungsten catalyst formation upon application of alkali treatment

Precursor	Methanol (mL)	Reaction time (min)	Drying Condition	Annealing					Alkali Treatment		
				Ramp rate (°C/min)	Gas	Flow (sccm)	T (°C)	Time (hr)	Chemical	Molar (M)	Time (hr)
VB = 0.2000 g WCl ₆ = 0.0813 g	10	5	60°C, 1 hr	10	NH ₃	100	650	2	KOH	1.5	24
		10									
		15									
		20									
		60									
		5									
		10									
		15									
		20									
		60									

mixing. Once the reaction was complete, tungsten metal complexes were added to the Vulcan black solution, which had been dispersed for 1 hour. As a result, the sample underwent RTA for annealing. The setup for the tungsten complex ion reaction is shown in Table 2. During the process, some samples received further alkali treatment. Samples that underwent annealing were treated with 1.5 M alkali solution and stirred for 24 and 48 hours (see Table 3). When mixing was finished, the sample was centrifuged at 12,000 rpm for 30 minutes. The supernatant was discarded, and the precipitate was washed with an equal volume of methanol and deionised water. This process was repeated three times, after which the sample was placed in a convection incubator for further analysis.

3. RESULTS AND DISCUSSION

Stoichiometric control is crucial for the formation of a single-atom catalyst [11]. It influences phase transition and stability through the thermodynamic driving force, resulting in a disorder-to-order phase transition. According to diffusion theory, high temperatures lead to increased energy barriers for atoms and diffusing support. Therefore, the stoichiometric ratio will act as a reference for developing single-atom catalysts. To achieve a single-atom catalyst, the number of tungsten atoms or concentration plays a crucial role in understanding the properties of this type of catalyst. This is primarily due to the high concentration of tungsten, which can lead to the formation of a tungsten crystal structure during the reaction with Vulcan black and subsequent annealing, as observed in our initial experiment on the Pt:W mol ratio. Therefore, the weight of Vulcan black and W was calculated according to a Pt: W mol ratio of 17:1. For example, in experiment number 1, 0.0504 grams of Vulcan black contained 5.2×10^{-5} mol of Pt. Thus, the weight of WCl_6 required was 0.0114 g to supply 2.9×10^{-6} mol of W from 1 mL of a stock solution. Accordingly, the mol ratio of Pt to W was maintained at 17:1.

The annealing temperature and duration were varied to screen the optimum condition to create a single-atom catalyst. In experiments 1, 2, and 3, the temperatures were 650°C, 700°C, and 750°C, respectively, with an annealing time of 4 hours. For experiments 4, 5, and 6, the annealing time was reduced to 2 hours to assess whether the X-Ray diffraction (XRD) spectra changed after this process. The XRD spectra shown in Figure 1 was plotted to examine phase purity and structural properties resulting from the annealing treatment. The study was carried out on commercial Vulcan black Pt/C. This sample was subjected to a reaction with tungsten complex ions and Pt/C, both with and without annealing treatments of 2 hours and 4 hours at temperatures of 650°C, 700°C, and 750°C. Regarding the effect of temperature, the XRD spectra exhibited a broad peak at lower temperatures and a sharper peak at higher temperatures. The low intensity of the XRD spectra indicates a low degree of crystallinity.

An increase in temperature led to changes in crystal phases, as evidenced by the growth in crystallinity and the altered aggregation pattern. High temperatures are associated with increased surface energy and a greater tendency for larger

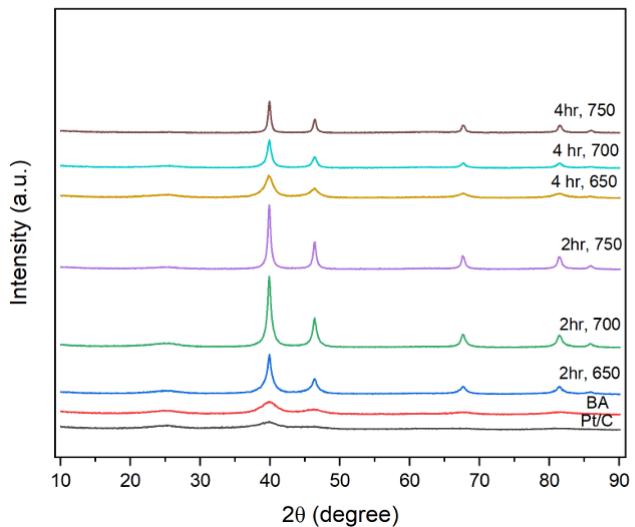


Figure 1. XRD spectra during the annealing process at temperatures of 650, 700 and 750°C, and the annealing was operated at 2 and 4 hours, respectively. Pt/C denoted as Vulcan black XC72 R, and BA is the sample without undergoing annealing.

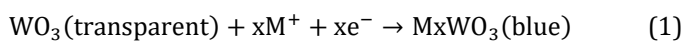
Pt clustering. Regarding annealing time, it was observed that no new crystal structures formed at 2 hours, even when the process was extended to 4 hours. However, a relatively high intensity was detected at 700°C and 750°C compared to 4 hours of annealing, which showed different spectra at 650°C as the duration increased. Consistent with the structure of Pt, all samples displayed peaks at 39.7°, 67.5°, and 46.1°, corresponding to the diffraction planes of (111), (200), and (220), respectively [12]. In samples containing tungsten complexes, including those before annealing and all samples subjected to the annealing process, peaks for W_2C were observed at 40° and 46°. Since the diffraction planes for Pt and WC are close in proximity, the spectra in XRD are often convoluted, which contributes to higher intensities across all samples when Pt/C is combined with tungsten complexes.

Additionally, we also observed WC spectra that can be acquired at a peak of 84°, contributed by the diffraction matrix (201) [11, 13]. From the XRD diffraction plane, it is clear that the sample that has not undergone annealing has a broader peak compared to the annealed sample, indicating a temperature effect on the phase structure and a different formation of the crystalline structure. High energy during annealing causes Pt atoms and W complexes to form clusters, thereby facilitating the development of a crystalline structure.

According to Han and coworkers, who studied the formation pathway of the Fe-Pt intermetallic compound, they observed that the annealing temperature is crucial for Fe diffusion, enabling the formation of ordered catalyst nanostructures in industrial applications [14]. Based on their findings regarding Fe diffusion and the development of an ordered nanostructure, it is evident that low temperature annealing at 450°C results in Pt aggregation into clusters on the carbon support. However, this temperature may not provide enough energy for Fe to diffuse and anchor as an active site. When the annealing

temperature increases to 650°C, it supplies sufficient energy for Fe atoms to diffuse into Pt clusters, potentially filling vacant sites within the nanostructure and on the Pt clusters, thus activating the single-atom Fe sites. Excessively high annealing temperatures can lead to the growth of polycrystalline material. In the case of Pt-Fe, when the temperature surpasses 950°C, an ordered Pt-Fe structure or alloy forms. Therefore, a suggested temperature range for complete elemental Fe diffusion during annealing might be between 650°C and 750°C, promoting the development of active single-atom catalyst sites.

Further investigation into the formation of single-atom tungsten catalysts was carried out to examine the reaction time of the single-atom precursor and the support material. Nishio and Toshio, who studied electrochromic thin films of tungsten oxide, prepared tungsten chloride and ethanol as starting materials and found that the reaction exhibited electrochromic behaviour where tungsten chloride transformed into tungsten oxide, switching from transparent to blue. This indicates the formation of tungsten methoxide ($\text{W}(\text{OCH}_3)_6$) and other tungsten alkoxides [15]. The involved reaction is shown in Equation 1 [16]:



Theoretically, during the reaction, methanol acts as both a solvent and a reactant for forming alkoxide precursors, which facilitate replacing chloride ligands with ethoxy groups. It converts into a methoxide ion, which then reacts with tungsten to form tungsten methoxide. This tungsten methoxide, present in a clear solution, serves as a single-atom precursor that further reacts with Pt/C to anchor as the support material and creates a single-atom active site. During the process, it was observed that the methoxide ion can change the colour to a blue solution, which is not desirable as a single-atom precursor. Since the reaction can continue further, it is necessary to control the stability of the methoxide ion. Therefore, to investigate the tungsten complex ions, the solution was analysed at different temperature settings, ranging from 5 minutes to 60 minutes.

In a smaller-scale reaction involving atomic processes, a rapid reaction rate is usually essential for the reaction to occur. For example, in precipitation, combustion, and polymerisation, poor mixing reduces the effectiveness of the reaction rate due to reagent depletion in the reaction [14]. Therefore, the use of ultrasound mixing in both water and viscous liquids creates intense micromixing through acoustic cavitation and acoustic streaming, leading to faster and more effective mixing at the molecular level compared to mechanical stirring [17]. Hence, micromixing was studied, and two samples were prepared: one through ultrasonic mixing, and the other served as the control. The ultrasonic sample was sonicated for 30 seconds, whereas the control was mechanically mixed. Table 4 summarises observations for both. At 0-minute, initial observations showed that the sonicated sample produced a white solution, whereas the control turned yellow after complete

mixing (Figure 2a). Within 15 minutes, the sonicated sample changed from white to clear, with no precipitation, while the control developed into a clear solution with a slightly muted white-yellow precipitate at the bottom. It was expected that the reaction of WCl_6 and methanol would convert WO_3 and M^+ as soon as the solution became transparent. However, precipitate was produced in the control sample during the reaction. By 60 minutes, both samples began turning blue, indicating the formation of tungsten bronzes. The clear solution was anticipated to undergo annealing before being transformed into tungsten bronzes.

Table 4. Single-atom tungsten catalyst formation upon application of Alkali treatment

Description	Sonicate	No Sonicate
Minute 15	Change in white solution	Change in white with precipitate on bottom layer
Minute 27	Clear	Clear with white precipitate
Minute 30	Clear	Clear with white precipitate
Minute 45	Clear	Clear with white precipitate
Minute 50	Clear	Started to appear blue precipitate
Minute 60	Turned blue	Turned blue

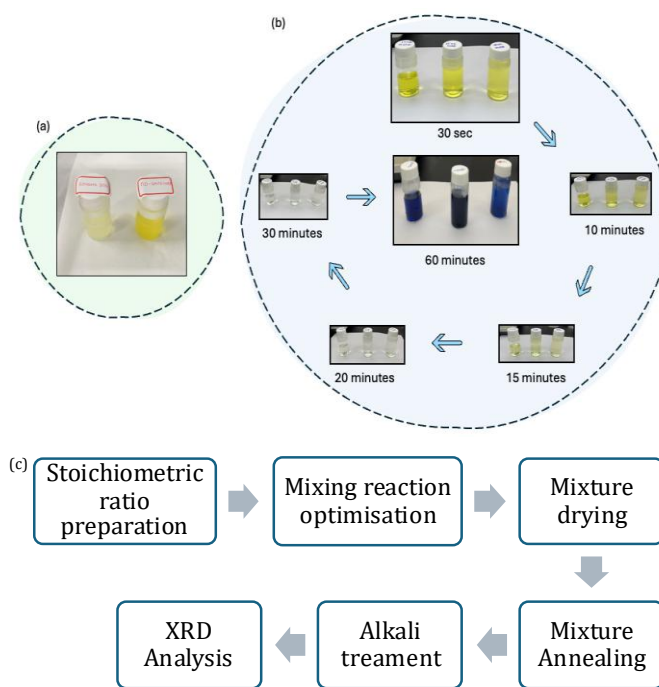


Figure 2. Images for single-atom tungsten precursors.
 (a) Micromixing experimental works. Left: ultrasonic sample sonicated for 30 seconds. Right: control sample that was mechanically mixed. (b) Images of reaction time for the formation of tungsten alkoxide as a single-atom tungsten precursor.
 (c) Process flow of SACs synthesis with XRD analysis

Additionally, Figure 2(b) displays observations when different volumes of methanol solution (10 mL, 15 mL, and 20 mL) are used to determine whether adding methanol affects the complexity of tungsten alkoxide production. All samples with different methanol volumes are supplemented with the same weight of WCl_6 . When WCl_6 is added to methanol, a yellow solution begins to turn blue, resulting in a darker appearance compared to the solutions with 15 mL and 20 mL, indicating a faster formation of tungsten bronzes and a higher yield. Based on this observation, the methanol volume was set at 10 mL.

Multiple catalysts were synthesised and analysed using XRD. The XRD spectra of the following substance, with the effect of reaction time that produces tungsten alkoxide from WCl_6 and methanol, were elucidated based on catalyst growth in Figure 3. Pt/C samples were made from fresh Vulcan black, which undergoes no treatment. Therefore, the XRD spectra for Pt/C showed a broad diffraction peak at 25° , indicating a graphitic carbon plane (002) for carbon support [18]. The diffraction peak indexed at 40° showed a distinction for Pt (111) [19]. As for the other sample, it involved incorporating WCl_6 with methanol, followed by drying and annealing. Additionally, samples were subjected to alkali treatment after annealing, a process that removes oxide layers from metal precursors and enhances the active site that promotes electronic delocalisation [20, 21]. Therefore, the diffraction peak for different reaction times yields distinct diffraction peaks, indicating the formation of tungsten with varying complexity. However, the pattern for XRD diffraction in minutes 5, 10, and 15 shows a similarity in peak position, indicating the presence of tungsten complex ions in a similar manner. However, the diffraction angle has a sharper peak at minute 5 compared to minutes 10 and 15, indicating that the reaction remained in a cloudy solution when it precedes drying and annealing, hence resulting in a lower formation of tungsten alkoxide.

The XRD spectra for 20 and 60 minutes showed a sharper peak, indicating a greater growth of atoms based on

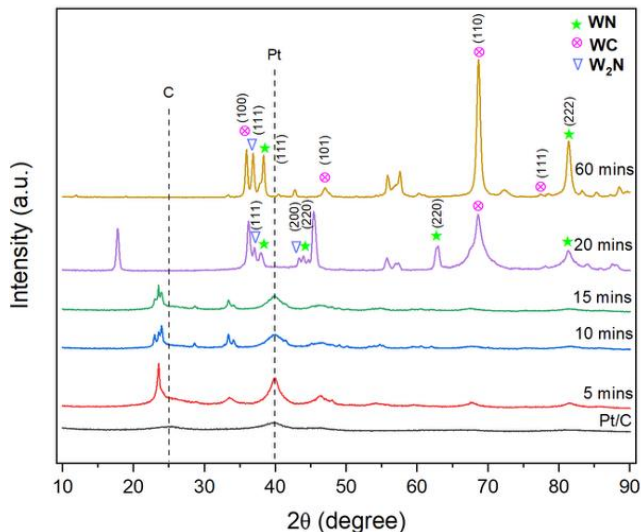


Figure 3. XRD spectra on the growth of tungsten on Pt/C. The reaction was studied for the tungsten complex ion at 5, 10, 15, 20, and 60 minutes

diffraction planes in the sample. The diffraction peaks had more indices, with a sharper peak and higher intensity, suggesting a more developed crystalline structure and a more ordered atomic arrangement [22]. For example, diffraction two theta at 38, 47, 70 and 78 indicated WC plane at (100), (101), (110) and (111) [23] while tungsten nitride (WN) exhibited at diffraction 34, 43 and 82 for plane (111), (200) and (222) [24]. Besides, the WN_2 crystal structure diffracted at 37 and 43 for planes (111) and (200) [24]. Generally, the other remaining peaks have similarity to tungsten trioxides [25]. The resultant is a variant of crystalline structures that is mainly due to tungsten complexes formed at minute 60, as supported by the colour change to a blue solution, indicating the formation of complex ions and tungsten bronzes, which contribute to the low yield of WO_3 and M^+ . Hence, the by-product in the tungsten precursor gained energy and aggregated to form a cluster, eventually creating an ordered structure.

4. CONCLUSIONS

The strategy for designing the process to produce single-atom tungsten catalysts was discussed, focusing on the annealing process, particularly in terms of temperature and duration. Additionally, the reaction that generates tungsten complex ions plays a crucial role in the aggregation and growth of atoms during annealing. A key factor that may accelerate the reaction for tungsten iron complexes identified in this experiment is ultrasonic mixing, as the reaction has the potential for rapid atomic-scale transformation. The mixing of tungsten (VI) chloride and methanol, using both ultrasonic and mechanical methods, revealed notable differences in the formation of tungsten alkoxide. The stoichiometric ratio is vital in studying the formation of a single-atom tungsten catalyst, including the volume of methanol, which may influence the formation of tungsten alkoxide and its by-products, evidenced by precipitation at the bottom of the solution. This is supported by the XRD spectra, which display different diffraction peaks at various reaction times, indicating the development of the crystal structure. Reactions at 10 and 15 minutes showed broader diffraction peaks with relatively low intensity, suggesting the possibility of single-atom tungsten formation.

ACKNOWLEDGMENTS

Authors thank Yung-Tin Pan, National Tsing Hua University for his support.

REFERENCES

- [1] H. Li, X. Qin, K. Wang, T. Ma, and Y. Shang, "Insight into metal-based catalysts for heterogeneous peroxyomonosulfate activation: A critical review," *Separation and Purification Technology*, vol. 333, p. 125900, 2024, doi: 10.1016/j.seppur.2023.125900.
- [2] Y. Zhang *et al.*, "Research on the resistance of catalysts for selective catalytic reduction: Current progresses and future perspectives," *Journal of Cleaner Production*, vol. 434, p. 139920, 2024, doi: 10.1016/j.jclepro.2023.139920.

[3] C. Xie, Z. Niu, D. Kim, M. Li, and P. Yang, "Surface and Interface Control in Nanoparticle Catalysis," *Chemical Reviews*, vol. 120, no. 2, pp. 1184–1249, 2020, doi: 10.1021/acs.chemrev.9b00220.

[4] S. Chen, F. Xiong, and W. Huang, "Surface chemistry and catalysis of oxide model catalysts from single crystals to nanocrystals," *Surface Science Reports*, vol. 74, no. 4, p. 100471, 2019, doi: 10.1016/j.surfrep.2019.100471.

[5] H. S. Taylor, "A theory of the catalytic surface," *Proceedings of the Royal Society of London. Series A, Containing Papers of a Mathematical and Physical Character*, vol. 108, no. 745, pp. 105–111, 1925, doi: 10.1098/rspa.1925.0061.

[6] H. Wang, T. Yang, J. Wang, Z. Zhou, Z. Pei, and S. Zhao, "Coordination engineering in single-site catalysts: General principles, characterizations, and recent advances," *Chem*, vol. 10, no. 1, pp. 48–85, 2024, doi: 10.1016/j.chempr.2023.08.014.

[7] B. Qiao *et al.*, "Single-atom catalysis of CO oxidation using Pt₁/FeO_x," *Nature Chemistry*, vol. 3, no. 8, pp. 634–641, 2011, doi: 10.1038/nchem.1095.

[8] S. Li *et al.*, "Single-atom photo-catalysts: Synthesis, characterization, and applications," *Nano Materials Science*, vol. 6, no. 3, pp. 284–304, 2024, doi: 10.1016/j.nanoms.2023.11.001.

[9] L. Liu and A. Corma, "Metal Catalysts for Heterogeneous Catalysis: From Single Atoms to Nanoclusters and Nanoparticles," *Chemical Reviews*, vol. 118, no. 10, pp. 4981–5079, 2018, doi: 10.1021/acs.chemrev.7b00776.

[10] J. Ding *et al.*, "Asymmetrically coordinated cobalt single atom on carbon nitride for highly selective photocatalytic oxidation of CH₄ to CH₃OH," *Chem*, vol. 9, no. 4, pp. 1017–1035, 2023, doi: 10.1016/j.chempr.2023.02.011.

[11] X. Han *et al.*, "In-situ atomic tracking of intermetallic compound formation during thermal annealing," *Nature Communications*, vol. 15, no. 1, p. 7200, 2024, doi: 10.1038/s41467-024-51541-0.

[12] O. L. Li, Z. Shi, H. Lee, and T. Ishizaki, "Enhanced Electrocatalytic Stability of Platinum Nanoparticles Supported on Sulfur-Doped Carbon using in-situ Solution Plasma," *Scientific Reports*, vol. 9, no. 1, p. 12704, 2019, doi: 10.1038/s41598-019-49194-x.

[13] J. Hu *et al.*, "Preparation of spherical WC–W₂C composite powder via noble metal-free catalytic electroless nickel plating for selective laser melting," *Materials Research Express*, vol. 6, no. 12, p. 125627, 2020, doi: 10.1088/2053-1591/ab6533.

[14] S. Som *et al.*, "Dopant distribution and influence of sonication temperature on the pure red light emission of mixed oxide phosphor for solid state lighting," *Ultrasonics Sonochemistry*, vol. 28, pp. 79–89, 2016, doi: 10.1016/j.ultsonch.2015.07.003.

[15] H. Kang *et al.*, "Temperature-dependent electrochromic cycling performance of solution-processed WO₃ films," *Nanoscale*, vol. 17, no. 35, pp. 20135–20147, 2025, doi: 10.1039/D5NR02842F.

[16] K. Nishio and T. Tsuchiya, "Electrochromic thin films prepared by sol-gel process," *Solar Energy Materials and Solar Cells*, vol. 68, no. 3–4, pp. 279–293, 2001, doi: 10.1016/S0927-0248(00)00362-7.

[17] X. Zhu, R. S. Das, M. L. Bhavya, M. Garcia-Vaquero, and B. K. Tiwari, "Acoustic cavitation for agri-food applications: Mechanism of action, design of new systems, challenges and strategies for scale-up," *Ultrasonics Sonochemistry*, vol. 105, p. 106850, 2024, doi: 10.1016/j.ultsonch.2024.106850.

[18] D. Rathod *et al.*, "Design of an 'all solid-state' supercapacitor based on phosphoric acid doped polybenzimidazole (PBI) electrolyte," *Journal of Applied Electrochemistry*, vol. 39, no. 7, pp. 1097–1103, 2009, doi: 10.1007/s10800-008-9764-3.

[19] I. C. Halalay, S. Swathirajan, B. Merzougui, M. P. Balogh, G. C. Garabedian, and M. K. Carpenter, "Anode Materials for Mitigating Hydrogen Starvation Effects in PEM Fuel Cells," *Journal of The Electrochemical Society*, vol. 158, no. 3, p. B313, 2011, doi: 10.1149/1.3530796.

[20] X. Chen, W. Liu, Y. Sun, T. Tan, C. Du, and Y. Li, "KOH-Enabled Axial-Oxygen Coordinated Ni Single-Atom Catalyst for Efficient Electrocatalytic CO₂ Reduction," *Small Methods*, vol. 7, no. 3, 2023, doi: 10.1002/smtd.202201311.

[21] A. Rujiwatra, N. Thammajak, T. Sarakonsri, R. Wongmaneerung, and S. Ananta, "Influence of alkali reagents on phase formation and crystal morphology of hydrothermally derived lead titanate," *Journal of Crystal Growth*, vol. 289, no. 1, pp. 224–230, 2006, doi: 10.1016/j.jcrysgro.2005.10.118.

[22] C. F. Holder and R. E. Schaak, "Tutorial on Powder X-ray Diffraction for Characterizing Nanoscale Materials," *ACS Nano*, vol. 13, no. 7, pp. 7359–7365, 2019, doi: 10.1021/acsnano.9b05157.

[23] M. Obradovic, B. Babic, A. Kowal, V. Panic, and S. Gojkovic, "Electrochemical properties of mixed WC and Pt-black powders," *Journal of the Serbian Chemical Society*, vol. 73, no. 12, pp. 1197–1209, 2008, doi: 10.2298/JSC08121970.

[24] A. H. Abdelhameed and W. Jacob, "Deposition of thermally stable tungsten nitride thin films by reactive magnetron sputtering," *Surface and Coatings Technology*, vol. 375, pp. 701–707, 2019, doi: 10.1016/j.surfcoat.2019.07.046.

[25] H. Zhang *et al.*, "Synthesis of uniform octahedral tungsten trioxide by RF induction thermal plasma and its application in gas sensing," *CrystEngComm*, vol. 15, no. 7, p. 1432, 2013, doi: 10.1039/c2ce26514a.